

# Characteristic Variability Time Scales of Long Gamma-Ray Bursts

Rong-Feng SHEN

*Particle Astrophysics Center, Institute of High Energy Physics,*

*Chinese Academy of Sciences, Beijing, 100039, P. R. China*

*shenrf@mail.ihep.ac.cn*

Li-Ming SONG

*Particle Astrophysics Center, Institute of High Energy Physics,*

*Chinese Academy of Sciences, Beijing, 100039, P. R. China*

*songlm@mail.ihep.ac.cn*

(Received ; accepted )

## Abstract

We determine the characteristic variability time scales ( $\Delta t_p$ ) of 410 bright and long GRBs, by locating the peaks of their Power Density Spectra defined and calculated in the time domain. We find that the averaged variability time scale decreases with the peak flux. This is consistent with the time dilation effect expected for the cosmological origin of GRBs. We also find that the occurrence distribution of the characteristic variability time scale shows bimodality, which might be interpreted as that the long GRB sample is composed of two sub-classes with different variability time scales. However, we find no difference for some other characteristics of these two sub-classes.

**Key words:** cosmology: observations — gamma rays: bursts — gamma rays: theory

## 1. Introduction

The isotropy of GRB directions and the deficiency of weak bursts suggest a cosmological origin of GRBs (Meegan et al. 1992), which has been confirmed by the detections of GRB afterglows (Costa et al. 1997; van Paradijs et al. 1997; Metzger et al. 1997; Kulkarni et al. 1998). An energy release of  $\sim 10^{51} - 10^{53}$  ergs (assuming no beaming) implied by the cosmological origin makes them to be outstanding events in the universe.

According to the most popular “fireball” model (Piran 1999), the observed  $\gamma$  rays are emitted when an ultra-relativistic flow is converted to radiation. It has been suggested that the energy conversion occurs either due to the interaction with the external medium (“external shocks”) (Rees & Mészáros 1992) or due to collisions within the flow (“internal shocks”) (Rees

& Mészáros 1994).

The progenitors of GRBs (“central engine”) remain the most mysterious since they are hidden from direct observations. The most popular models are mergers of two compact objects (NS-NS merger or NS-BH merger) or collapse of massive stars. Currently it is difficult to distinguish them from observations. It is also likely that more than one type of progenitors could give rise to GRBs, and overall GRBs may comprise different sub-classes corresponding to different progenitors. The most well known classes are the short and the long classes separated at  $T_{90} \sim 2s$ , arising from their bimodal duration ( $T_{90}$ ) distribution (Kouveliotou et al. 1993). In recent years, a few works are devoted to reclassification of GRBs using multivariate analysis, which yield three sub-classes (Mukherjee et al. 1998; Balastegui et al. 2001).

About 2000 GRBs<sup>1</sup> have been detected and recorded by the Burst And Transient Source Experiment (*BATSE*) on board the *Compton Gamma-Ray Observatory*. They have a complicated and irregular time profiles which vary drastically from one burst to another. Recent studies in internal shock paradigm show that the observed complicated temporal structures are directly associated with the activity of central engine (Kobayashi et al. 1997). The observed variability provides an interesting clue as to the nature of GRBs (Piran 1999).

Observationally, the light curve of a burst is consisted of successive pulses, which may be the fundamental emission units. Many people have decomposed light curves into pulses using model-dependent fitting (Norris et al. 1996) or peak finding selection (Nakar & Piran 2002; McBreen et al. 2001) and analysed the temporal properties of the resulted pulses, such as rise time, decay time, FWHM, and time interval between the neighbouring pulses. However, the real time profiles are so irregular that many pulses are overlapping and unseparable, prohibiting a clear decomposition of those pulses.

In this paper we adopt a different approach. We calculate the power density spectra (PDS) in the time domain for 410 bright long bursts, and regard the time scale corresponding to the maximum of the PDS as the time scale of typical variations in the profile, and thus define it as characteristic variability time-scale of the burst. We then study the distribution of the characteristic variability time scale and the correlation between the time scale with the GRB intensity.

## 2. PDS in The Time Domain

Many authors have calculated the PDSs of GRBs with the Fourier transformation (Beloborodov et al. 1998; Beloborodov et al. 2000; Pozanenko & Loznikov 2000). However, Fourier analysis cannot replace the direct variability study in the time domain. Except for the periodic and quasi-periodic processes there is no direct correspondence between a structure in the Fourier spectrum and the physical process taking place at a certain time scale. The power

---

<sup>1</sup> <http://gammaray.msfc.nasa.gov/batse/grb/catalog/current/>

density at a given Fourier frequency can result from contributions from different processes on different time scales.

Without using the Fourier transformation, a new technique for timing analysis in the time domain has been proposed recently (Li 2001; Li & Muraki 2002). Quantities characterizing temporal properties, e.g., power density, coherence, and time lag, can be defined and calculated directly in the time domain with this technique.

Following Li (2001), the variation power in a light curve  $x(k)$  is defined as

$$P(\Delta t) = \frac{Var(x)}{(\Delta t)^2} = \frac{\frac{1}{N} \sum_{k=1}^N (x(k) - \bar{x})^2}{(\Delta t)^2},$$

where  $x(k), k = 1, \dots, N$ , is a counting series obtained from a time history of observed photons with a time step  $\Delta t$ , and  $\bar{x} = \sum_{k=1}^N x(k)/N$  is the average counts. The power  $P(\Delta t)$  represents the contribution from the variation at all time scales  $\geq \Delta t$ . The power density  $p(\Delta t)$  can be defined in the time domain as the rate of change of  $P(\Delta t)$  with respect to the time step  $\Delta t$ . From two powers  $P(\Delta t_1), P(\Delta t_2)$  at two time scales  $\Delta t_1, \Delta t_2$  ( $\Delta t_2 > \Delta t_1$ ), the power density at time scale  $\Delta t = (\Delta t_1 + \Delta t_2)/2$  is evaluated approximately by

$$p(\Delta t) = \frac{P(\Delta t_1) - P(\Delta t_2)}{\Delta t_2 - \Delta t_1}.$$

For a noise series where the  $x(k)$  follow the Poisson distribution, the noise power is given by

$$P_{noise}(\Delta t) = \frac{Var(x)}{(\Delta t)^2} = \frac{\langle x \rangle}{(\Delta t)^2},$$

and the noise power density at  $\Delta t = (\Delta t_1 + \Delta t_2)/2$  is

$$p_{noise}(\Delta t) = \frac{P_{noise}(\Delta t_1) - P_{noise}(\Delta t_2)}{\Delta t_2 - \Delta t_1}.$$

The signal power density can then be defined as

$$p_{signal}(\Delta t) = p(\Delta t) - p_{noise}(\Delta t).$$

### 3. Data Reduction

We use the *BATSE* Concatenated 64-ms Burst Data summed over energy channel II and III (50 - 300 keV), and we utilize the results of background fitting for 64-ms Burst Data from [http://cosscc.gsfc.nasa.gov/batseburst/sixtyfour\\_ms/bckgnd\\_fits.html](http://cosscc.gsfc.nasa.gov/batseburst/sixtyfour_ms/bckgnd_fits.html). In order to reduce the influence of background, one would like to cut the light curve with a window neatly including the whole burst. We define and use the “ $T_{100}$  window” where  $T_{100} = T_{90}/90\%$ . The window is obtained by extending the  $T_{90}$  window forward for  $0.05T_{90}$  and backward for  $0.05T_{90}$  respectively.

Since we are interested in using the PDS to investigate the variation power distribution over a large range of time scales, short bursts are not suitable for calculating the PDS, except that their durations are long compared with the timing resolution. We thus select bursts only with  $T_{100} > 15s$ . To avoid large Poisson fluctuations in the light curve, we exclude dim bursts

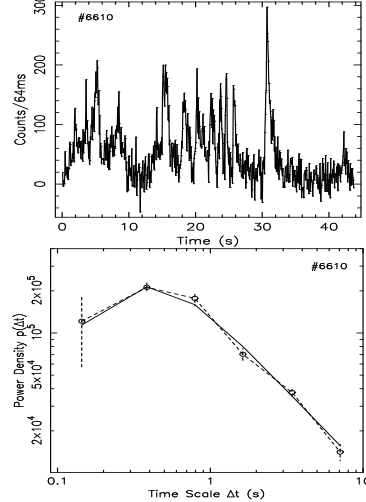


**Fig. 1.** Time profiles of a burst (*upper panel*) and its PDS calculated in the time domain (*lower panel*). Solid line is the broken power law model fit to the calculated PDS.

with peak count rates  $< 250$  counts per 64ms bin. This two criteria give a sample of 478 bursts from the *BATSE* Current Catalog<sup>2</sup>. Then we calculate the PDS of each burst in the time domain with the algorithm described in Section 2.

#### 4. PDS Calculation

For an individual burst, the power densities are calculated at time scales  $\Delta t$  arranged at equal intervals in the logarithmic space. To avoid fluctuations in the PDS, we binned PDS with approximately equal number of data points in each time scale bin and the uncertainties of the data are derived from the binning.

Most of the bursts' PDSs show a “bump” shape. The bump-shape indicates that the variation peaks at specific time scale; we regard the peak time scale  $\Delta t_p$  as the characteristic variability time scale of the burst.

To improve the accuracy of  $\Delta t_p$ , we fitted the PDS with a broken-power-law model  $p(\Delta t) = \frac{(\Delta t/P_1)^{P_2+P_3}}{(\Delta t/P_1)^{P_2} + (\Delta t/P_1)^{P_3}} P_4$ ; the fit is acceptable for most bursts. The characteristic variability time scale  $\Delta t_p$  is determined from the peak location of the fitted PDS curve. Fig. 1 gives an example of a burst's time profiles and its PDS.

#### 5. Characteristic Variability Time Scales

##### 5.1. $\Delta t_p$ for A Simulated Time Series

Does  $\Delta t_p$  really reflect the variability time scale of the typical variation? How is  $\Delta t_p$  correlated with the sizes of pulses if we consider the burst is composed of stochastic pulses? To

<sup>2</sup> <http://gamma-ray.msfc.nasa.gov/batse/grb/catalog/current/>

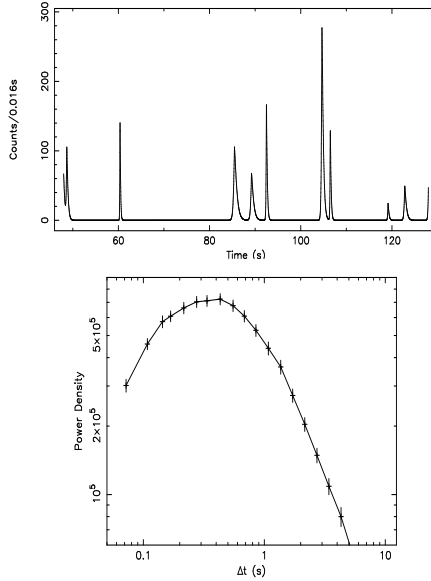


**Fig. 2.** A simulated time series (*upper panel*) and the calculated PDS (*lower panel*). The stochastic pulse parameters:  $\langle \ln(\tau_r) \rangle = -2.0$ ,  $\tau_d/\tau_r = 2.5$ .

answer these questions, we simulated a long stochastic time series with 16 ms time resolution and 4800 s duration. The time series are divided into 100 segments and power densities at different time scales are calculated for each segment. The resulted PDS is obtained by averaging the PDSs over 100 segments. The pulse model are taken from Norris et al. (1996), with the pulse shape

$$\begin{aligned} I(t) &= A \exp[-(|t - t_{max}|/\tau_r)^\nu], \quad t < t_{max}, \\ &= A \exp[-(|t - t_{max}|/\tau_d)^\nu], \quad t > t_{max}, \end{aligned}$$

where  $t_{max}$  is the time of pulse's peak,  $A$  is pulse amplitude,  $\nu$  is the “peakedness” parameter, and  $\tau_r$  and  $\tau_d$  are the rise and decay time constants, respectively.

We assumed that the interval between the neighbouring pulses is exponentially distributed with a mean value of 10 s,  $A$  is uniformly distributed within 10 - 200 counts/0.016s,  $\nu = 1.2$ , the rise time constants  $\tau_r$  are a Log-Normal distribution with standard deviation  $\sigma(\ln \tau_r) = 0.5$ , and the decay-to-rise ratio  $\tau_d/\tau_r$  is a constant. We defined the *pulse rising time*  $t_r$  as the duration that the intensity  $I(t)$  increases from 5% $A$  to the peak. We then choose different values for mean  $\langle \ln \tau_r \rangle$  and decay-to-rise ratio  $\tau_d/\tau_r$  to simulate the time series, and calculate the PDS in the time domain. The characteristic variability time scale  $\Delta t_p$  are determined from the peak of the PDS. Shown in Fig. 2 are a simulated time series and the calculated PDS, respectively. Fig. 3 plots  $\Delta t_p$  vs.  $\langle t_r \rangle$ . Fig. 3 shows that  $\Delta t_p$  is truly the variability time scale of typical variations, and is sharply correlated with the rising time  $t_r$  of the typical pulses.

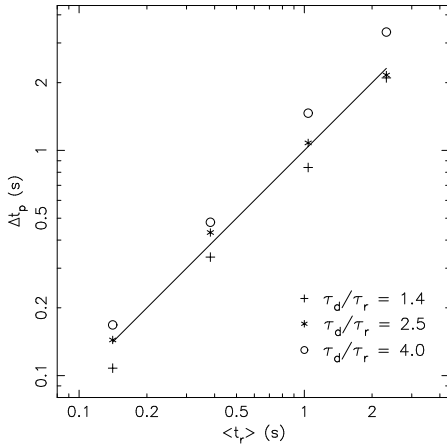


**Fig. 3.** Characteristic variability time scales  $\Delta t_p$  vs.  $\langle t_r \rangle$ , for simulated time series. See definition of  $t_r$  in the text. Solid line represents  $\Delta t_p = \langle t_r \rangle$ . Note the correlation between  $\Delta t_p$  and the average rising time  $\langle t_r \rangle$  of the stochastic pulses.

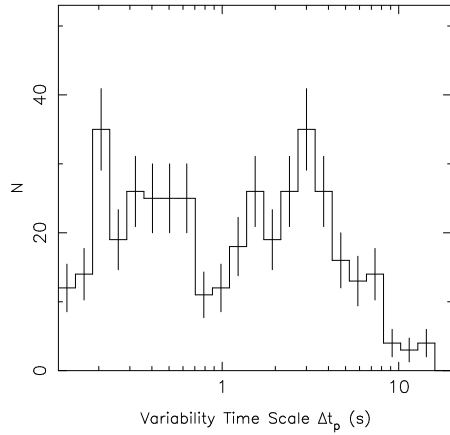


**Fig. 4.** Histogram distribution of characteristic variability time scales for 410 bright long bursts.

### 5.2. Distribution of $\Delta t_p$

Among the PDS samples, 63 PDS samples keep rising till the smaller time-scale limit where the PDS can be calculated, without showing decrease. It means that, the characteristic time scales of those bursts are smaller than or equal to the smaller time-scale limit, whereas they cannot be determined yet. After discarding the 63 samples and 5 badly fitted ( $\chi^2/\nu > 50$ ) samples, we obtain  $\Delta t_p$  for 410 bursts. Fig. 4 plots their histogram distribution; it is a bimodal distribution with the demarcation at  $\Delta t_p \sim 1s$ .

To investigate the reliability of the bimodality, we performed the *chi-squared test* (Press et al. 1992) for the differences between the distribution data and a known uniform distribution in the range of  $\Delta t_p \sim 0.1 - 8.0s$  where 19 bins were included. The mean of the

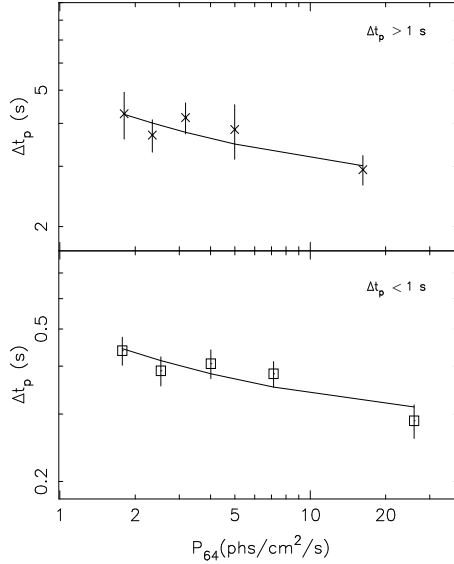


**Fig. 5.**  $\Delta t_p$  vs. brightness distribution for the slow variable group ( $\Delta t_p > 1\text{s}$ ) and fast variable group ( $\Delta t_p < 1\text{s}$ ). Each bin includes equal number of samples. Solid lines are the best-fit model predictions.

**Table 1.** Fitted results for time dilation in the slowly variable group ( $\Delta t_p > 1\text{s}$ ) and the fast variable group ( $\Delta t_p < 1\text{s}$ ). The estimated uncertainties of  $\Delta t_0$  and the luminosity correspond to the 90% confidence level.

Group	$\Delta t_0$ (s)	Peak luminosity ( $10^{50}\text{ergs/s}$ )	$z_{min}$	$z_{max}$
$\Delta t_p > 1\text{s}$	$2.30(\pm 0.18)$	$7.56(\pm 2.81)$	$0.28(\pm 0.16)$	$0.85(\pm 0.32)$
$\Delta t_p < 1\text{s}$	$0.256(\pm 0.004)$	$5.52(\pm 0.36)$	$0.13(\pm 0.11)$	$0.72(\pm 0.15)$

uniform distribution was set to that of the data sets. The test gives a *chi-squared probability*  $Q(\chi^2|\nu) = 1.437 \times 10^{-4}$ , where the small value of  $Q(\chi^2|\nu)$  indicates a significant difference between these two distributions. The bimodal distribution of  $\Delta t_p$  indicates that bursts of  $\Delta t_p > 1\text{s}$  and  $\Delta t_p < 1\text{s}$  may belong to two GRB sub-classes respectively.

### 5.3. Time Dilation Test

If a GRB occurs at a cosmological distance, then every structure in the time profile will be stretched by a factor  $1+z$  due to the expanding universe, where  $z$  is the red shift. Therefore, we should observe that the dimmer bursts have larger characteristic variability time scales than the brighter bursts do, assuming bursts at different cosmological distances are “standard candles” with the same intrinsic characteristic variability time scale.

According to the bimodal distribution of  $\Delta t_p$ , we divide the bursts into  $\Delta t_p > 1\text{s}$  group and  $\Delta t_p < 1\text{s}$  group, and plot in Fig. 5 the distribution of the mean of  $\Delta t_p$  in 5 brightness bins for each group, where brightness is represented by  $P_{64}$ , the peak flux measured at the 64 ms time scale. Both groups show that the averaged  $\Delta t_p$  decreases with the brightness, consistent with the cosmological origin of GRBs.

To quantitatively test the time dilation effect, we fitted the  $\Delta t_p$  vs. brightness distributions with a model prediction; the model is described in the Appendix. Table 1 lists the fitting results for  $\Delta t_p > 1s$  group and  $\Delta t_p < 1s$  group, respectively, in a standard  $\Omega = 1, \Lambda = 0$  cosmology, with the normalized Hubble constant  $h$  set to 0.75. The luminosity is a multiplication of the peak photon number luminosity and the assumed mean photon energy, 150 keV. The time dilation factors  $(1 + z_{max})/(1 + z_{min})$  derived for the  $\Delta t_p > 1s$  group and the  $\Delta t_p < 1s$  group are 1.46( $\pm 0.27$ ) and 1.52( $\pm 0.20$ ), respectively.

## 6. Discussion

We have calculated PDSs of 410 bright long bursts in the time domain, and determined their characteristic variability time scales by locating the peaks of their PDSs. The distribution of  $\Delta t_p$  is a bimodal distribution with the demarcation at  $\Delta t_p \sim 1s$ . GRBs may be divided naturally into two groups, a fast variable group and a slowly variable group.

Following Kobayashi et al. (1997) and Piran (1999), in the internal shock paradigm, the emitted radiation from each collision between two relativistic shells will be observed as a single pulse, whose time scale depends on the cooling time, the hydrodynamic time, and the angular spreading time. In most of cases, the electron cooling time is much shorter than the latter two. The hydrodynamic time scale is determined by the time that the shock crosses the shell, whose width is  $d$ . Calculation reveals that this time scale (in the observer's rest frame; so does  $d$ ) is of order of the light crossing time of the shell, that is:  $d/c$ . If the collision of the shells takes place at a larger radius  $R$ , angular spreading (Sari & Piran 1997) affects the time scale of the pulse. If the distance between shells is  $\delta$ , the resulted angular spreading time for the pulse is  $\sim \delta/c$ . If  $\delta > d$ , the observed variability time scale will be determined by angular spreading. In any case, the observed temporal structure is directly associated with the variability of the “central engine”, and the observed time scale is proportional to the size of the ejected wind or the separation between the winds. Consequently it is likely that the observed time scale is correlated with the size of the progenitor.

Our results about existence of a fast variable group and a slowly variable group may indicate that the bright long bursts comprise two sub-classes generated from different sizes of ejected winds or distances between winds, or from different sizes of the progenitors. Both groups show the trend that the characteristic variability time scale decreases with the brightness of the burst, consistent with the cosmological time dilation effect. We fitted the data to a model for both the fast variable group and the slowly variable group respectively. The smaller values of  $z_{max}$  and time dilation factors, compared with previous results (Norris et al. 1994; Che et al. 1997), may be because our sample does not include more weak bursts.

The authors thank S. N. Zhang, T. P. Li, W. F. Yu, F. J. Lu and J. L. Qu for their useful discussions and valuable advices. We thank S. N. Zhang for carefully reading through the manuscript. This work is supported by the Special Funds for Major State Basic Research Projects of China, and has made use of data obtained from the High Energy Astrophysics Science Archive Research Center (HEASARC) provided by NASA's Goddard Space Flight Center.

## Appendix. Model Prediction for Time Dilation

The cosmological time dilation effect will stretch every time structure of GRBs, if they are at cosmological distances. Assuming GRBs have the same characteristic variability time scale  $\Delta t_0$ , we should observe

$$\Delta t = \Delta t_0(1+z). \quad (\text{A1})$$

Since red shift  $z$  is unknown, the observed peak flux  $P$  [phs s<sup>-1</sup> cm<sup>-2</sup>] is used to express  $z$  under the “standard candle” assumption. For simplicity, we introduce the peak photon number luminosity  $L_n$  [phs s<sup>-1</sup>] as the standard luminosity of GRBs, without considering the photon energy redshift. For a standard Friedmann cosmology ( $\Omega = 1, \Lambda = 0$ ), the luminosity distance is

$$d_L = 2R_0(1+z - \sqrt{1+z}), \quad (\text{A2})$$

where  $R_0 = c/H_0 = 9.25h^{-1} \times 10^{27}$  cm, and  $h = H_0/100$  is the normalized Hubble constant. Then the observed peak flux is

$$P = \frac{L_n}{4\pi d_L^2}. \quad (\text{A3})$$

Combining equations (A2) and (A3) yields

$$1+z = \frac{1}{2} \left[ 1 + 0.3h\sqrt{L_{n56}/P} + \left( 1 + 0.6h\sqrt{L_{n56}/P} \right)^{1/2} \right], \quad (\text{A4})$$

where  $L_{n56} = L_n/10^{56}$  is the normalized peak photon number luminosity. Therefore from equation (A1) we obtain

$$\Delta t = \frac{1}{2} \left[ 1 + 0.3h\sqrt{L_{n56}/P} + \left( 1 + 0.6h\sqrt{L_{n56}/P} \right)^{1/2} \right] \Delta t_0, \quad (\text{A5})$$

which can be compared with observations.

## References

- Balastegui A., Ruiz-Lapuente P., Canal R., 2001, MNRAS, 328, 283  
 Beloborodov A. M., Stern B. E., Svensson R., 1998, ApJ, 508, L25  
 Beloborodov A. M., Stern B. E., Svensson R. 2000, ApJ, 535, 158

- Che H., Yang Y., Wu M., et al., 1997, ApJ, 477, L69
- Costa E., Frontera F., Heise J., et al. 1997, Nature, 387, 783
- Kobayashi S., Piran T., Sari R., 1997, ApJ, 490, 92
- Kouveliotou C., Meegan C. A., Fishman G. J., et al., 1993, ApJ, 413, L101
- Kulkarni S. R., Djorgoski S. G., Ramaprakash A. N., et al. 1998, Nature, 393, 35
- Li T. P., 2001, Chin. J. Astron. Astrophys., 1, 313
- Li T. P., Muraki Y., 2002, ApJ, 578, 374
- McBreen S., Quilligan F., McBreen B., et al., 2001, A&A, 380, L31
- Meegan C. A., Fishman G. J., Wilson R. B., et al., 1992, Nature, 355, 143
- Metzger M. R., Djorgovski S. G., Kulkarni S. R., et al., 1997, Nature, 387, 878
- Mukherjee S., Feigelson E. D., Babu G. J., et al., 1998, ApJ, 508, 314
- Nakar E., Piran T., 2002, MNRAS, 331, 40
- Norris J. P., Nemiroff R. J., Scargle J. D., et al., 1994, ApJ, 424, 540
- Norris J. P., Nemiroff R. J., Bonnell J. T., et al., 1996, ApJ, 459, 393
- Pozanenko A. S., Loznikov V. M., 2000, In: R. M. Kippen, R. S. Mallozi, G. J. Fishman, eds., Gamma-Ray Bursts: 5<sup>th</sup> Huntsville Symposium, AIP Conf. Proc. 526, New York: AIP, p. 220
- Piran T., 1999, Phys. Rep., 314, 575
- Press W. H., Teukolsky S. A., et al., 1992, Numerical Recipes in FORTRAN, 2nd ed., Cambridge: Cambridge University Press
- Rees M. J., Mészáros P., 1992, MNRAS, 258, 41
- Rees M. J., Mészáros P., 1994, ApJ, 430, L93
- Sari R., Piran T., 1997, ApJ, 485, 270
- van Paradijs J., Groot P. J., Galama T., et al. 1997, Nature, 386, 686